Lawrimore et al., http://www.jcb.org/cgi/content/full/jcb.201502046/DC1

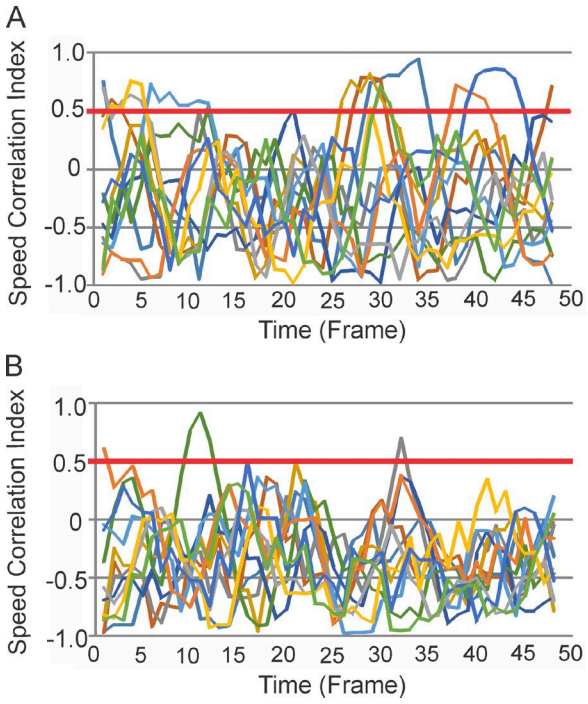

C

SCI above 0.5	Untreated	Benomyl
Total	8%	1%
2 Consecutive	7%	1%
5 Consecutive	4%	0%

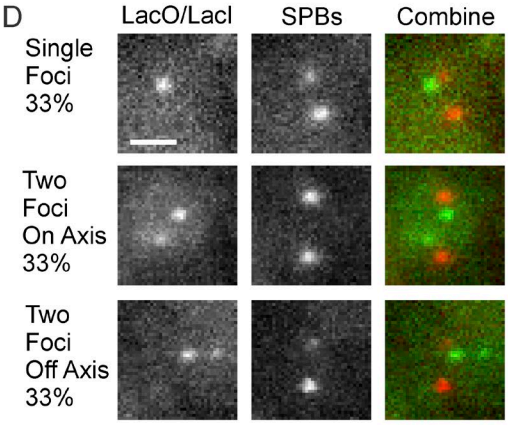

Figure S1. **Speed correlation index analysis and orientation of pericentric chromatin separation.** (A) Plot of speed correlation index (SCI) over time for untreated cells containing a 6.8-kb LacO/LacI-GFP array. Each line represents individual GFP foci with the corresponding SPB motion subtracted. Red bar indicates SCI of 0.5, the threshold used for assigning directed motion. SCI was calculated using a window size of 4 frames. The x-axis denotes progression of averaged frames over the ~2.5-min of the time course of analysis. The negative skew in SCI is similar to that observed for actin filament motion in the nucleus and attributed to properties of particles imbedded in a viscoelastic medium such as the nucleoplasm (Weber et al., 2010; Belin et al., 2013; B) Plot of SCI over time for benomyl-treated cells. The data shown in A and B are from 6 experiments (two foci each) with SCI values for $n = 12$ foci in both A and B. (C) Summary of the percentage of time SCI was >0.5 in total, >0.5 for two consecutive time points, or >0.5 for 5 consecutive time points for untreated and benomyl-treated cells. (D) Representative images of yeast containing an ndc10-2 mutation at restrictive temperature. Cells contain labeled pericentric chromatin (LacO/LacI-GFP 1.7 kb from CEN11) in green and SPBs (Spc29-CFP) in red. Pericentric foci in cells with two SPBs appeared as a single focus, two on-axis foci, or two off-axis foci. The percentage of the population for each phenotype is shown (total, $n = 15$). Bar, 1 µm.

A

	Foci (n = 33)	Stretched All Spindle Lengths (n = 31)	Stretched Spindles< 2 µm (n = 20)	Stretched Spindles > 2 µm (n = 11)
Average Radial Displacement (nm)	78 ± 49	47 ± 49	64 ± 50	17 ± 29
Average Axial Displacement (nm)	436 ± 108	684 ± 353	455 ± 112	1100 ± 246

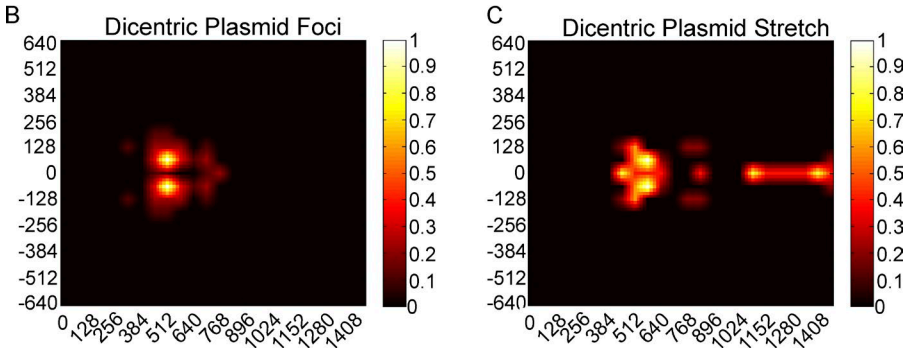

Figure S2. **Heat map analysis of unreplicated, dicentric plasmids.** (A) Table summarizing the mean radial and axial displacement of the TetR-GFP signals that appear as foci or elongated filaments. Heat maps of TetR-GFP signals that appear as foci (B) and elongated filaments (C).

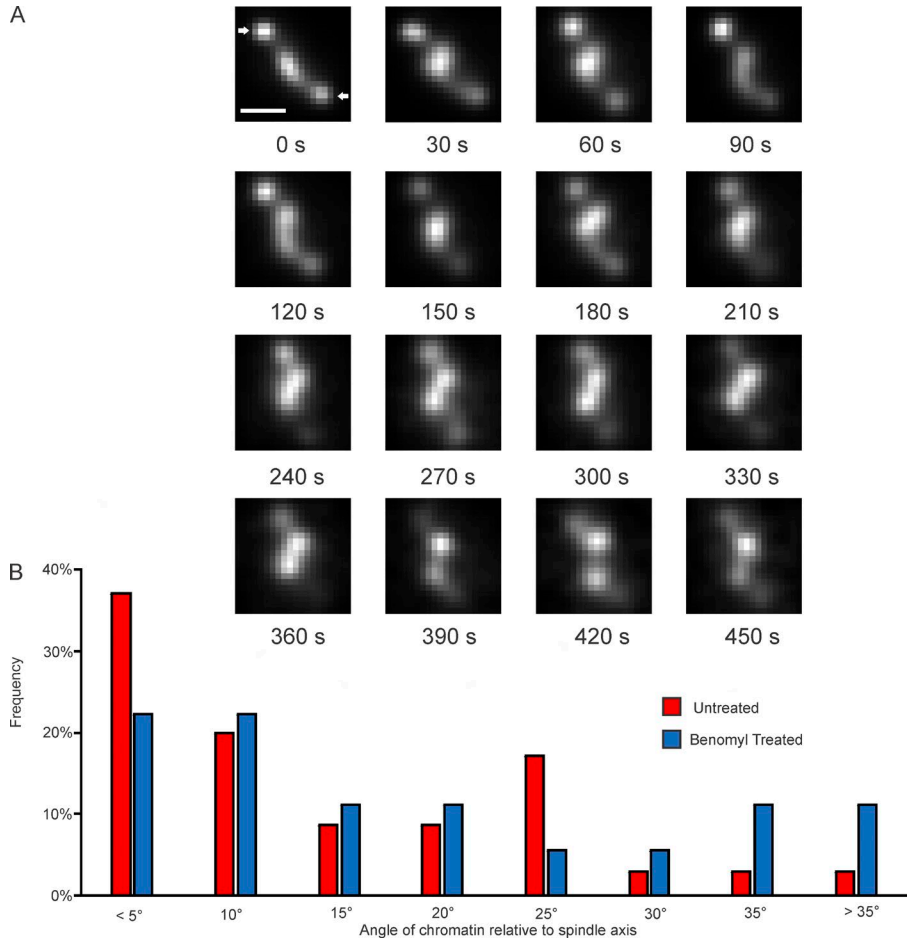

Figure S3. **Fluctuation and trajectory of dicentric plasmids relative to the mitotic spindle axis.** (A) Fluorescent images of configurational states of the dicentric plasmid in metaphase. Deconvolved single-plane images of cells containing a single dicentric plasmid at 30-s intervals up to 450 s are shown. Spindle poles appear as diffraction-limited spots indicated with arrows. Bar, 0.5 μm. (B) Angular distribution of elongated dicentric plasmids in 0.5–1.8-μm spindles from individual cells in a population. Angles represent the difference between the trajectories of the primary chromatin axis relative to the spindle axis (defined by the two spindle poles, indicated with arrows). The percentages are calculated using data from multiple experiments (untreated, n = 35 arrays; benomyl treated, n = 18 arrays). Red, untreated; blue, benomyl treated.

Table S1. **One-dimensional radii of confinement and effective spring constants**

Name	Sample size (number of coordinates)	Radius of confinement		Effective spring constant		Levene's test parallel vs. perpendicular p-value
		Parallel to axis	Perpendicular to axis	Parallel to axis	Perpendicular to axis	
6.8 kb (Chr XV) Untreated	525	594	349	1.5×10^{-4}	4.2×10^{-4}	4×10^{-18}
6.8 kb (Chr XV) Benomyl	861	483	335	2.2×10^{-4}	4.6×10^{-4}	1×10^{-12}
6.8 kb (Chr XV) Azide	441	130	110	3.0×10^{-3}	4.3×10^{-3}	0.01
240 kb (Chr II) Untreated	609	793	716	8.1×10^{-5}	1.0×10^{-4}	0.06

Radii and effective spring constants calculated using population variance in a single dimension.

Table S2. **Directional analysis of step size relative to spindle axis**

Measurement	WT (3-s interval)	Benomyl (3-s interval)	WT (30-s interval)	Benomyl (30-s interval)
Average step size[a] (nm)	81 ± 54	63 ± 39	177 ± 110	156 ± 104
Average displacement parallel to axis[b] (nm)	51 ± 46	37 ± 32	143 ± 116	112 ± 98
Average displacement perpendicular to axis[+] (nm)	46 ± 43	41 ± 33	85 ± 77	89 ± 82

[a]The one-dimensional step sizes of LacO/LacI-GFP foci were calculated using Pythagorean Theorem. WT, 3 s, *n* = 698; Benomyl, 3 s, *n* = 1,601; WT, 30 s, *n* = 525; Benomyl, 30 s, *n* = 861.
[b]How far each focus traveled in a single dimension, parallel and perpendicular to the spindle axis, during each step. WT, 3 s, *n* = 710; Benomyl, 3 s, *n* = 1,616; WT, 30 s, *n* = 820; Benomyl, 30 s, *n* = 500.

Table S3. **Percent of directed motion of pericentric chromatin in bub1Δ**

Minimum displacement	Untreated (*n* = 13 foci)		Benomyl (*n* = 11 foci)	
	Parallel	Perpendicular	Parallel	Perpendicular
nm				
300	29%	3%	14%	4%
350	20%	3%	11%	4%
400	14%	0%	7%	2%

Table S4. **Percent of directed motion of GFP separation**

Minimum displacement	Untreated Stu2^{CU} (*n* = 4 cells)	Copper added Stu2^{CU} (*n* = 4 cells)	Benomyl Stu2^{CU} (*n* = 3 cells)	Untreated WT (*n* = 11 cells)	Benomyl WT (*n* = 8 cells)
nm					
300	50%	17%	4%	7%	2%
350	41%	15%	2%	6%	2%
400	35%	14%	0%	6%	0%

References

Belin, B.J., B.A. Cimini, E.H. Blackburn, and R.D. Mullins. 2013. Visualization of actin filaments and monomers in somatic cell nuclei. *Mol. Biol. Cell.* 24:982–994. http://dx.doi.org/10.1091/mbc.E12-09-0685

Weber, S.C., A.J. Spakowitz, and J.A. Theriot. 2010. Bacterial chromosomal loci move subdiffusively through a viscoelastic cytoplasm. *Phys. Rev. Lett.* 104:2381010.1103/PhysRevLett.104.238102. http://dx.doi.org/10.1103/PhysRevLett.104.23810220867274